

# Preparation, structural and NLO-optical characterization of LB-molecular films from asymmetric Bent-Core liquid crystals

P. García-Vázquez<sup>a</sup>, O.G. Morales-Saavedra<sup>b,\*\*</sup>, M.D.P. Carreón-Castro<sup>a,\*</sup>, and G. Pelzl<sup>c</sup>

<sup>a</sup>*Instituto de Ciencias Nucleares, Universidad Nacional Autónoma de México,*

*Circuito Exterior Ciudad Universitaria, Apartado Postal 70-543, Coyoacán, 04510, Cd. Universitaria, México D. F. México,*

*\*Tel: (+52-55)56.22.46.74/75/85, Fax: (52-55)56.22.47.07.*

*e-mail: pilar@nucleares.unam.mx*

<sup>b</sup>*Centro de Ciencias Aplicadas y Desarrollo Tecnológico, Universidad Nacional Autónoma de México,*

*CCADET-UNAM. Circuito Exterior S/N, Ciudad Universitaria, Apartado Postal 70-186, C.P. 04510, México D.F., México,*

*\*\*Tel: (+52-55)56.22.86.02, Ext. 1109, Fax: (5255) 56.22.86.37.*

*e-mail: omar.morales@ccadet.unam.mx*

<sup>c</sup>*Institut für Physikalisches-Chemie, Martin Luther University,*

*Halle-Wittenberg, Mühlpforte 1. D-06108 Halle. Germany.*

Received 5 March 2014; accepted 19 August 2014

Molecular mono- and multilayered films of a polar asymmetric bent-core (“banana-shaped”) liquid crystalline (LC) compound with hydrocarbon end-chains were prepared by the Langmuir-Blodgett (LB) technique. Langmuir films were characterized by surface pressure isotherms and Brewster angle microscopy (BAM). Likewise, LB-films deposited onto glass substrates were characterized by UV-VIS spectroscopy, the optical second harmonic generation (SHG) technique and atomic force microscopy (AFM). Results show that the asymmetric structure of bent-core liquid crystals may promote an unstable multi-layered ( $n > 10$  LB-layers) LB-architecture which leads to a rapid collapse of Z-type arrangements, giving rise to a drastic decrease of the nonlinear optical (NLO) properties and film quality. Indeed, measurements evidence a tolerable and uniform molecular coverage on the glass substrates with anisotropic orientational distribution for a moderate number of layers only ( $n \leq 10$  LB-layers); where, according to NLO-experimental data, the net molecular polarization is aligned outward the substrate layer. This observation leads us to implement a simplified model based on the monomeric rod-like approximation, in order to estimate significant NLO-tensorial components and an effective molecular hyperpolarizability  $\beta_{\text{eff}}$ -coefficient along the polar axes of the 2D-polar LC-compound within the mechanical stable LB-monolayer arrangements.

**Keywords:** Langmuir-Blodgett films; non linear optics; liquid crystals; Bent-Core mesogens.

Películas moleculares mono y multicapa a base de un compuesto asimétrico líquido cristalino (LC) con propiedades polares (del tipo “banana”) y conteniendo cadenas terminales hidrocarbonadas, fueron preparadas sobre sustratos de vidrio mediante la técnica de depósito Langmuir-Blodgett (LB). Previo al depósito, las películas de Langmuir fueron caracterizadas mediante isoterma de presión superficial y microscopía de ángulo de Brewster (BAM). Asimismo, las películas depositadas LB fueron caracterizadas por espectroscopía UV-VIS, por medio de la técnica de generación del segundo armónico óptico (SHG) y por microscopía de fuerza atómica (AFM). Los resultados muestran que estos compuestos LC asimétricos promueven la formación de estructuras LB multicapa altamente inestables (para  $n > 10$  depósitos LB del tipo Z), lo cual conlleva a un rápido colapso de estos sistemas y a una drástica disminución de sus propiedades ópticas no lineales (NLO) y de la calidad estructural de las películas. En efecto, los resultados experimentales evidencian sistemas multicapa razonablemente homogéneos con una distribución molecular anisotrópica para sistemas LB con al menos un número moderado de depósitos (para  $n \leq 10$ ). De acuerdo a mediciones de ONL, el momento dipolar neto de estos sistemas está alineado hacia afuera del plano del sustrato; esto nos llevó a la implementación de un modelo simplificado (para el sistema mono-capa con mayor estabilidad mecánica), basado en la aproximación de moléculas tipo “rodillo”; esto para la evaluación de las componentes tensoriales más significativas de las propiedades de ONL de estas moléculas, así como para la estimación del coeficiente de hiper-polarizabilidad molecular  $\beta_{\text{eff}}$  a lo largo del eje polar de este tipo de compuestos con estructura 2D.

**Descriptores:** Películas Langmuir-Blodgett; óptica no lineal; cristales líquidos; mesógenos banana.

PACS: 78.15.+e, 42.65.Ky, 78.66.-w.

## 1. Introduction

The recently re-discovered bent-core (banana-shaped) mesogens [1], represent a third subfield of thermotropic liquid crystals, because these molecules adopt a compact packing arrangement, that restricts rotational freedom and promotes their organization into different types of liquid crystalline phases, conventionally called phases B1, B2, B3, B4, etc. Most of these phases have smectic structure with a net polar-

ization in each layer, which could give chiral or achiral symmetries with interesting electro-optical (EO) and other physical properties, such as ferroelectricity, making these materials potentially suitable for relevant technological applications in organic devices [2-3]. Usually, organic functional materials have been processed in the form of films serving as active layers in devices; thus, studies concerning the film growth mechanism, the molecular ordering, and the overall film morphology are of prime importance for device design [4]. One

of the powerful sample preparation techniques for this purpose is the Langmuir-Blodgett (LB) technique. This technique, which involves the formation of a monolayer film on a water surface with subsequent transfer onto a solid substrate, is a viable route to produce active thin films with controllable thickness and architecture, which may be applied in molecule-based electrical and optical devices. Most importantly, the LB-technique is a powerful tool to investigate several optical and molecular ordering properties at the fundamental level, particularly in molecular monolayer systems.

Some research groups have demonstrated that it is possible to produce stable monolayer arrangements of two-dimensional (2D) banana-shaped mesogens and they have studied the dielectric, ferroelectric and antiferroelectric properties, the anisotropy as well as the orientational distribution of the corresponding molecular structures by surface second-harmonic generation, where the monolayer is transferred onto a glass substrate using the Langmuir-Blodgett (LB) technique [5-12]. Despite these efforts, there still exists a huge need of experimental data in order to better understand the alignment properties of these types of compounds in LB-systems; this is a difficult task due to the complexity of these mesogens and the number of imaginable configurations they can achieve in such structures. Thus, several experimental techniques should be implemented in order to better precise the molecular organization within the films, which is still more complicated for multilayer arrangements.

Recently, our group has proven that it is also possible to fabricate stable Z-Type multilayer arrangements of bent-core based LB-films suitable for quadratic nonlinear optical (NLO) characterizations, at least for a moderate number of layers (few dozens, [13]) implementing symmetric banana mesogens. Thus, the main scope of this work is, taking advantage of the LB-technique, to produce Langmuir monolayers and non-centrosymmetric Z-type Langmuir-Blodgett mono- and multilayer LB-arrangements from an asymmetric bent-core compound, deposited onto glass substrates. Hence, several physical properties from this kind of molecules could be investigated at a molecular level in low-range ordered systems; for instance, as active media for quadratic  $\chi^{(2)}$  NLO effects. Concretely, the studied bent-core compound consists of a central fragment constituted by a benzoyl derivative of a secondary cyclo amine, and presents an asymmetric molecular architecture since the length and chemical structure of the lateral monomeric units are different. This kind of compound and similar asymmetric structures were synthesized and characterized by the group of Prof. G. Pelzl and Prof. W. Weissflog from the *Institut für Physikalische Chemie* (at the Martin-Luther-Universität Halle-Wittenberg, Germany) [1,13-14] and by other research groups [15], respectively. With a particular compound of this family [14], we performed both the Langmuir film deposition and the subsequent mono- and multi-layer LB-deposition onto glass substrates. The corresponding film inspections were carried out via surface pressure isotherms combined with compression-expansion cycles (hysteresis) and Brewster angle microscopy

(BAM); the LB-films were also characterized according to AFM, UV-VIS spectroscopy and the second harmonic generation (SHG) technique, calibrated via the Maker fringes method. The NLO-measurements were carried out in order to achieve some insight into the molecular orientational distribution, but most importantly to provide experimental evidence toward the of fabrication of multilayer non-centrosymmetric structures with these types of asymmetric materials, suitable for quadratic NLO- and other optical-effects.

## 2. Materials and Experimental Methodology

### 2.1. Architecture of the implemented bent-core molecular structure

The studied banana-mesogen was provided by the Halle-group (Germany); this compound is schematically represented in Figs. 1/a-b and corresponds to compound Nr. 3 in Ref. [14]. This mesogen belongs to a new class of bent-core LC-material in which the central fragment consists of a benzoyl derivative of a secondary cyclo amine, where the bending of the molecule is not achieved by 1,3-substitution of a central aromatic ring as in common “banana”-mesogens, but by a carbonyl group linking the phenyl ring of one leg to the nitrogen of a piperazine ring which is part of the second leg of the mesogen. In this work, this compound is referred to as **ABL**C (asymmetric bent liquid crystal).

The studied compound exhibits a thermotropic behavior and the corresponding phases and transition enthalpies have already been reported in the literature [14]. The implemented dodecyloxy homologue 3 does not exhibit a nematic phase, so that only a smectic SmCP phase is directly formed at 215°C on cooling the isotropic liquid; the other monotropic crystalline (Cr) phase appears at 164°C. Furthermore, electro-optic studies reveal an antiferroelectric SmCPA ground state [14]. In fact, on a at the molecular level the structure of this

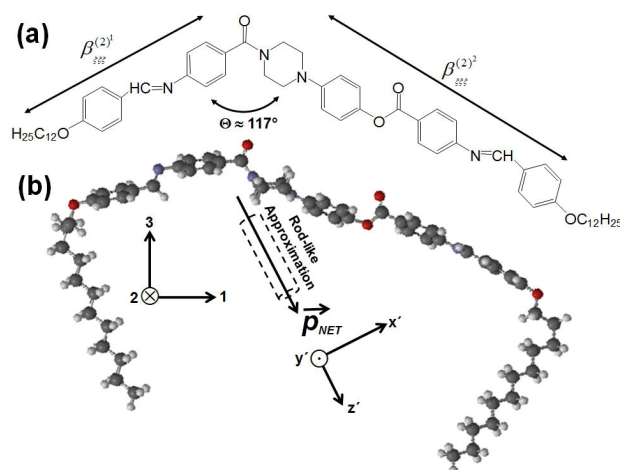


FIGURE 1. a-b) Molecular structure of the implemented ABLC “banana-shaped” compound (compound Nr. 3 in Ref. [14]).

banana-shaped compound shows a clear non-centrosymmetric density distribution of the conjugated  $\pi$ -electron-system, forming dipoles along the molecular wings and resulting in a permanent molecular dipole moment  $\vec{P}_{NET}$  which is vectorially located between these two main molecular axes. These properties give rise to polar order and are, in principle, equivalent to a non-centrosymmetric crystalline arrangement: a fully necessary condition for the occurrence of quadratic NLO/SHG-effects. Specifically, these properties are due to the presence of electro-donor and electro-acceptor systems linked together as bis-dipolar molecules: the presence of the amine atoms and the carboxyl- and oxy-groups on the molecular wings produce a net polarization within the molecular bent direction, making this compound an interesting candidate due to its asymmetric two-dimensional charge-transfer nature. Under this framework, molecular coordinate systems are also given in Figs. 1 in order to identify the main NLO-tensorial components as studied later on this paper. In fact, the first molecular hyperpolarizability  $\beta^{(2)}$  can be expressed in terms of the hyperpolarizabilities  $\beta_{\xi\xi\xi}^{(2)}$  of the one-dimensional monomeric units and the dihedral angle  $\Theta$  between these two monomers [5], where  $\xi$  is the direction of the charge transfer in each monomer. Recent studies have proven that such two-dimensional systems lead to the observation of important optical nonlinearities since the nonvanishing components along the conjugation length of the two benzylideneaniline wings produce large molecular hyperpolarizabilities [5,16-17]. Geometry optimizations of this structure were performed with the Spartan 04<sup>©</sup> (V1.0.0) molecular modeling package (see Fig. 1/b), in order to estimate the conformation occupied by this molecule at the water-air interface in Langmuir-films, corresponding to the molecular area given by the surface-pressure molecular area isotherm (see the next sections).

## 2.2. Preparation and characterization of Langmuir and LB-films

Data were collected using a Teflon trough and symmetrical hydrophobic barriers. The trough was set in a Plexiglas enclosure so as to be protected from drafts and dust; temperature was controlled to  $\pm 0.1^\circ\text{C}$ . All isotherms were taken at  $20^\circ\text{C}$ . The ultra-pure water ( $\rho = 18.2 \text{ M}\Omega \text{ cm}$ ) used for the sub-phase was obtained from a Milli-DI/simplicity 185 both from Millipore [18]. The spreading solution was prepared in HPLC grade chloroform (from Aldrich) at a specific concentration of  $1 \text{ mg mL}^{-1}$ . Monolayer studies were carried out with a KSV 5000 trough system 3 (KSV, Finland). A suitable amount of spreading solution was slowly spread onto the water surface by a microsyringe ( $50\text{-}100 \mu\text{L}$ ). After spreading, a monolayer was maintained for 10 minutes at room conditions for solvent evaporation; thereafter, it was symmetrically compressed with a barrier speed of  $10 \text{ mm min}^{-1}$ . The surface pressure measurements were performed via the Wilhelmy method. The stability of the monolayers was studied by repetitive compression-expansion pro-

cesses (hysteresis-loops) as long as the collapse pressure was not exceeded. The uniformity of prepared Langmuir films was monitored by BAM via a MiniBAM-Plus equipment from Nanofilm-Technology GmbH (Germany). The BAM system was equipped with a 30 mW laser source working at  $\lambda = 660 \text{ nm}$ , with variable incidence angles adjusted within the  $52\text{-}54^\circ$  interval. During these experiments, high resolution surface control images were acquired from an in-built CCD-camera. This device is connected to a NIMA trough (Model: 6222D, UK) to produce the molecular monolayers.

LB-film depositions were performed onto Corning-glass substrates of  $75 \times 25 \times 1 \text{ mm}^3$ . The substrates were successively treated with a sulphochromic mixture solution, ultra-pure water, then ethanol (Aldrich, reagent grade) and finally chloroform (Aldrich, reagent grade) and stored in clean-dry conditions before deposition. Z-type multilayer structures with  $n = 1, 5, 10, 20$ , and 40 layers were prepared by the vertical deposition method (extraction process only) at a target pressure in the range of  $10\text{-}16 \text{ mN m}^{-1}$  and a dipping speed of  $10 \text{ mm min}^{-1}$ , waiting 10 minutes between successive dipping cycles in order to evaporate the trapped sub-phase. The first deposit was aged for 24 h for drying. UV-Vis spectra of glass substrates covered with Langmuir monolayers were obtained with a CaryWin 100 Fast-Scan-Varian spectrophotometer using a glass slide without Langmuir monolayer as a reference.

Finally, the surface morphology of selected LB-films was analyzed by atomic force microscopy (AFM, Park AutoProbe CP equipment), where the acquisition of images was performed in non-contact mode with a rectangular cantilever (dLever<sup>TM</sup>) with a typical force constant of  $11 \text{ N m}^{-1}$  and a resonant frequency of  $40 \text{ kHz}$ , specifying the mechanical characteristics implemented during AFM-measurements.

## 2.3. Nonlinear optical SHG-characterization

Mono- and multi-layer non-centrosymmetric Z-type LB-film samples of the asymmetric bent-core compound ( $n = 1, 5, 10, 15, 20$  and 40) deposited onto glass substrates were studied as active media for quadratic  $\chi^{(2)}$ -nonlinear optical effects such as SHG. The SHG experimental device consists of a commercial Q-switched Nd:YAG Laser system (Surelite II from Continuum,  $\lambda_\omega = 1064 \text{ nm}$ , repetition rate of  $10 \text{ Hz}$  and a pulse width of  $\tau = 22 \text{ ns}$ ). Typical pulse energies of  $50 \mu\text{J}$  were filtered in order to irradiate the samples by means of a  $f = 50 \text{ mm}$  focusing lens, thus peak irradiances on the order of  $2 \text{ GW cm}^{-2}$  were achieved at the focal spot on the sample. The polarization of the input fundamental beam (S or P polarizing geometry) was selected by means of an IR-coated Glan-Laser polarizer and a  $\lambda/2$ -Quartz-retarder. A second polarizer was used as analyzer allowing the characterization of the SHG-signals. The second harmonic waves (at  $\lambda_{2\omega} = 532 \text{ nm}$ ) were detected by a sensitive photomultiplier tube behind interferential optical filters while the sample was slowly rotated around the z-axis within the  $-45^\circ$  -  $45^\circ$  interval. The SHG-device was calibrated by

means of an  $\alpha$ -quartz crystal, wedged along the  $d_{11}$ -direction ( $d_{11} = 0.64 \text{ pm V}^{-1} = 0.5\chi_{11}^{(2)}$ ), which is commonly used as a NLO-reference standard via the Maker fringes method [19-23]. All the NLO-measurements were performed at room conditions.

### 3. Results and Discussion

#### 3.1. Langmuir monolayer surface

Figures 2/a-b show the representative isotherm for compound **ABLC** and the respective hysteresis loops upon successive compression-expansion cycles, respectively. Here, the surface pressure measurements versus mean molecular area are shown. This method allows the description of the molecular arrangement at the air-water interface of the mesogen. Indeed, as shown in the representative isotherm (see Fig. 2/a), from 275 to  $91 \text{ \AA}^2 \text{ molecule}^{-1}$ , the interactions between the mesogens are rather poor, as in a gaseous phase, and the surface pressure remains almost zero. At  $91 \text{ \AA}^2 \text{ molecule}^{-1}$  the surface pressure begins to increase, from  $0 \text{ mN m}^{-1}$  up to  $12.8 \text{ mN m}^{-1}$  ( $54 \text{ \AA}^2 \text{ molecule}^{-1}$ ). In this region there is a

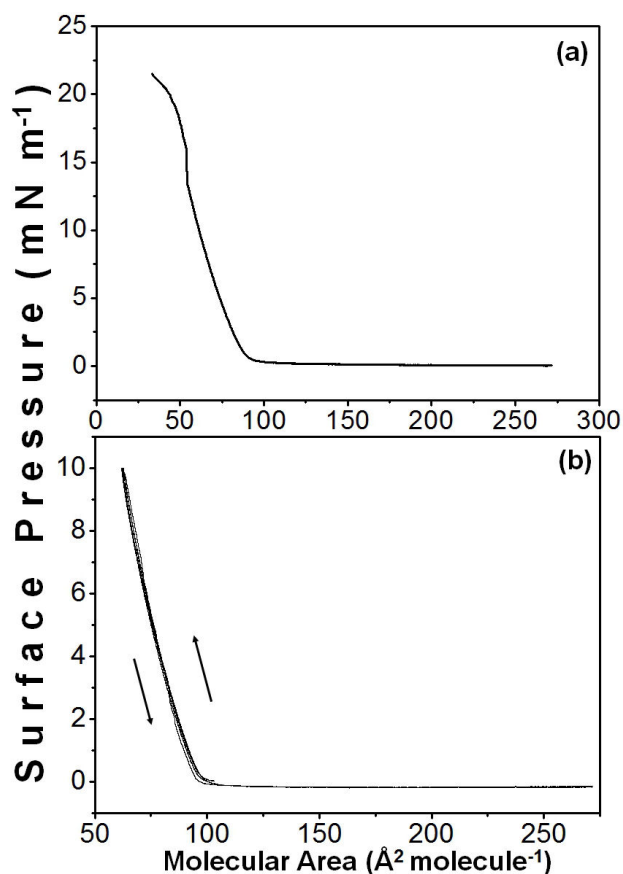


FIGURE 2. a) Surface pressure-molecular area isotherm, b) hysteresis cycles obtained for compound **ABLC**.

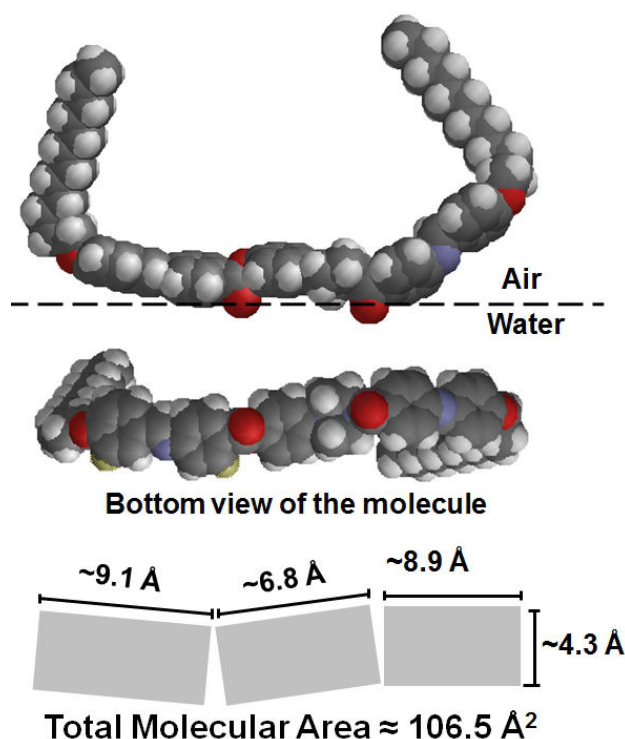


FIGURE 3. a) Molecular modeling optimized with Spartan 04<sup>©</sup> of **ABLC** at the air-water surface interface and bottom view of the molecule indicating the calculated molecular area within the condensed phase.

a phase transition of the molecules in order to get a compact arrangement of the Langmuir film. From this point on, the molecular area remains constant until the Langmuir film collapses at around  $13.5 \text{ mN m}^{-1}$ . The molecular area extrapolated to zero surface pressure is  $\sim 91 \text{ \AA}^2$ . The observed molecular area corresponds well to the calculated area, obtained based on the geometries optimized by Spartan 04<sup>©</sup> (see Fig. 3). It is suggested from this model, that the mechanical LB-deposition of this type of molecular film onto solid glass substrates would produce polar LB-layers, with the net polar molecular axis  $\vec{P}_{NET}$  pointing outwards from the substrate plane (in a perpendicular-close configuration). In fact, as shown in Fig. 3, the most probable conformation of the molecule at the air-water interface for the Langmuir monolayer indicates that the carbonyl groups tend to be inside the water due to their hydrophilic-group character, forming hydrogen bonds with water molecules. On the other hand the phenyl rings tend to be nearly flat with respect to the water surface and the aliphatic chains tend to be as far as possible from the water surface because of their hydrophobic character [24]. Finally, the obtained Langmuir films showed excellent reversibility upon successive compression-expansion cycles as long as the collapse pressure was not exceeded, which is evidenced by the similar shapes of the hysteresis-loops (Fig. 2/b), where no irregularities during the compression-expansion cycles are observable.

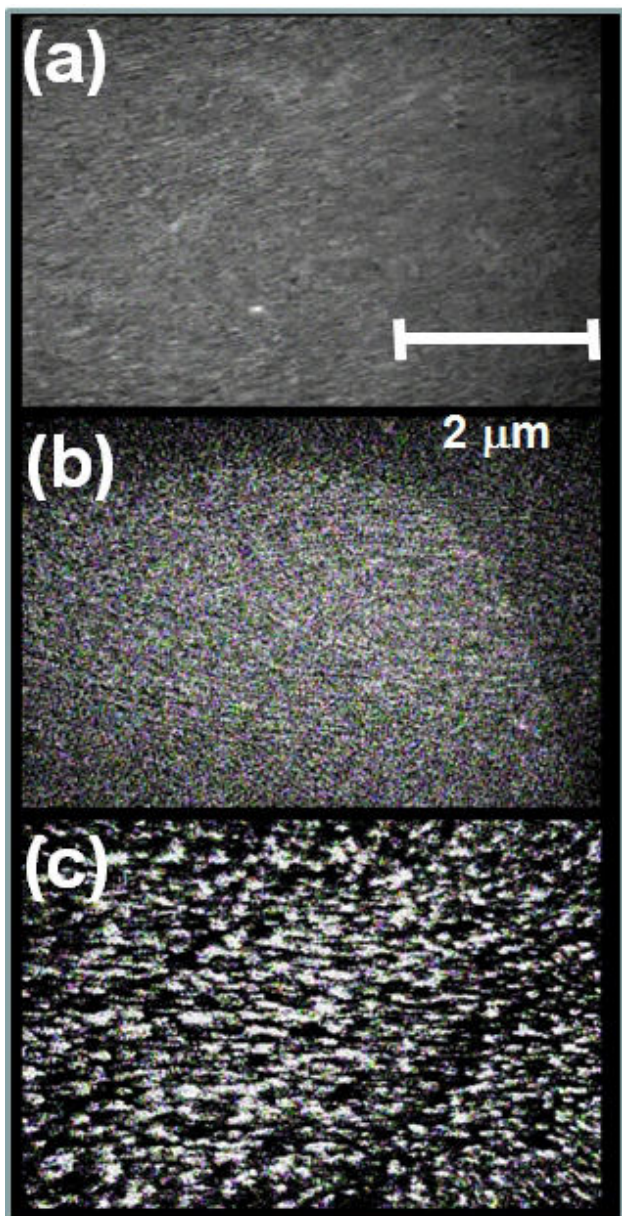


FIGURE 4. BAM images of the ABLC Langmuir monolayer recorded at different surface pressures: a)  $0 \text{ mN m}^{-1}$ , b)  $\sim 10 \text{ mN m}^{-1}$  and d)  $\sim 19 \text{ mN m}^{-1}$ .

Figures 4/a-c show a sequence of BAM-micrographs recorded at different surface pressures from the obtained Langmuir monolayer, which are useful to determine optimal pressure and molecular area conditions for subsequent LB-film depositions onto glass substrates. According to the discussions above, BAM observations recorded at different pressures reveal good quality of the Langmuir monolayer film. The region before compression consists of a homogeneous monolayer with very small holes but covering the whole aqueous surface (see Fig. 4/a). Upon decreasing the surface area by compression of the film, a condensed and packed phase is obtained, gradually revealing optimal conditions for mono- and multi-layer LB-deposition onto glass-substrates. The ob-

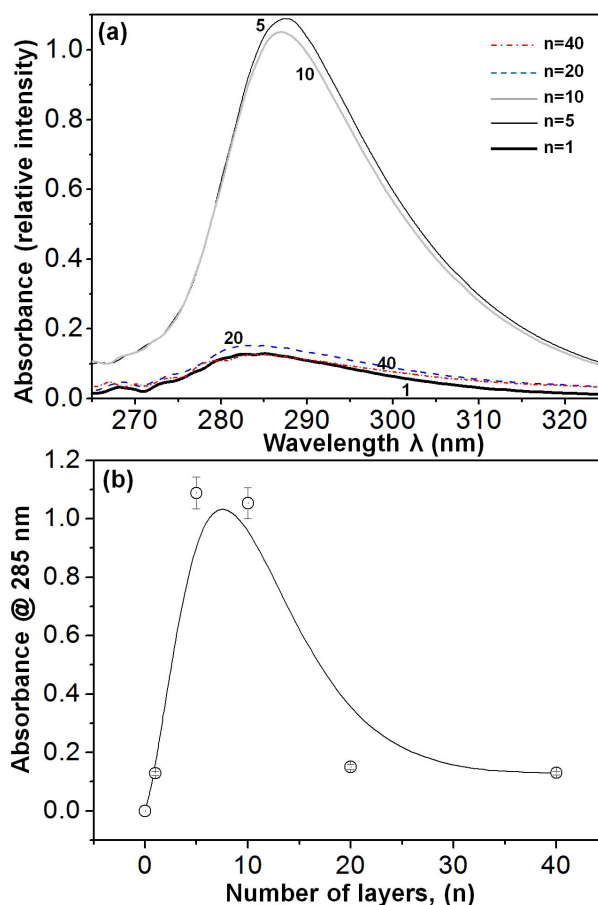


FIGURE 5. a) Absorption spectra of Z-type LB-films for compound ABCL ( $n = 1, 5, 10, 20$  and  $40$  layers). b) Absorption intensity at  $\lambda_{\text{max}} = 285 \text{ nm}$  as function of the number of layers ( $n$ ).

tained monolayer exhibits an increased texture roughness which could be associated with a change of the molecular tilt angles with respect to the water surface, or to the movement of the aliphatic chains towards the air phase ( $\sim 10 \text{ mN m}^{-1}$ , see Fig. 4/b). At a pressure of  $\sim 20 \text{ mN m}^{-1}$  (see Fig. 4/c), the formation of aggregates (isolated molecular islands) associated with the collapse and breakup of the film can be observed.

### 3.2. UV-VIS Spectroscopy monitoring of the LB-film deposition process

The Langmuir monolayers transferred at optimal conditions (as shown in Fig. 4/b) onto solid glass substrates and the subsequent multilayer depositions performed with a transfer ratio close to unity (ranging from 0.7 to 1.0) for a gradual increment of transfer pressure, were carefully monitored according to UV-Vis spectroscopy. As shown in Figs. 5/a-b, the absorbance dependence with the number of deposited layers  $n$  is reported. According to this figure, the SHG wavelength (at  $532 \text{ nm}$ ) is quite far from the absorbance peak ( $\lambda_{\text{max}} \approx 286 \text{ nm}$ ); thus, non-resonant experimental conditions for NLO-measurements are guaranteed. Here, a drastic decrease on the absorbance features can be observed for

$n > 10$  layers; this evident decrement of the absorptive properties occurring although the number of deposition cycles increases, indicate an unstable multilayered molecular ordering for this kind of asymmetric LC-mesogens. Indeed, as shown in Fig. 5/a, a broad absorbance spectrum with a maximum around 286 nm, characteristic of aromatic groups can be observed for all deposited mono- and multi-layer LB-samples. The absorbance does not increase linearly with increasing number of deposited layers; by contrast, after  $n = 5 - 10$ , the absorbance rapidly decreases with increasing number of deposited layers confirming a nonlinear and irregular growth of the multilayered LB-systems. This indicates a severe multilayer collapse and an inhomogeneous deposition of material after subsequent deposition cycles for this kind of bent-core compound (see Fig. 5/b). We argue that the asymmetry of the implemented mesogen play a key role and drastically influences their arrangement and packing within the LB multilayered structure: as the number of layers increases, a dense packing of the molecules becomes more difficult to achieve, creating hollows and fissures due to the weak Van der Waals molecular interactions and steric impediment of the aliphatic chains. This is followed by a drastic decrease of material accumulation after each deposition cycle, leading to structural disorder and a progressive disintegration of multilayer LB-arrangements. The latter arguments are supported, as explained below, via AFM and SHG-measurements.

### 3.3. AFM - LB film morphology

The variations of the microscopic surface morphology and roughness of the deposited LB-films were examined by AFM as shown in Fig. 6/a-d. Here, 3D-micrographs provide a small surface inspection ( $1 \times 1 \mu\text{m}$ ) of the nanostructured organization, topological arrangement, film roughness and quality of the LB-layers. A notable increase of the root-mean-square (rms)-roughness of the deposited films from 7.71 Å (for  $n = 1$ ) to 27.6 Å (for  $n = 40$ ) can be observed. According to AFM-inspections, in the case of deposited monolayer LB-films ( $n = 1$ ), the nanometric monomeric molecules agglomerate to generate a grain-like structure in the range of 2-6 nm (measured from amplified high-quality digitalized images), showing a homogeneous and nearly monomodal grain size distribution (with only a few defects) at large micrometric length-scale, which agrees well with the molecular dimensions of the bent-core compounds [1,12] (see Fig. 6/a). This arrangement shows the lowest rms-roughness (7.71 Å) and inter-grain porosity. For increasing LB-layer depositions ( $n = 10$ , Fig. 6/b), a clear change in the film morphology is observed: the agglomerates tend to grow forming huge granular structures in the range of 20 to 40 nm, showing an inhomogeneous surface but still a reasonably monomodal grain size distribution at the same micrometric length-scale. These arrangements show an in-

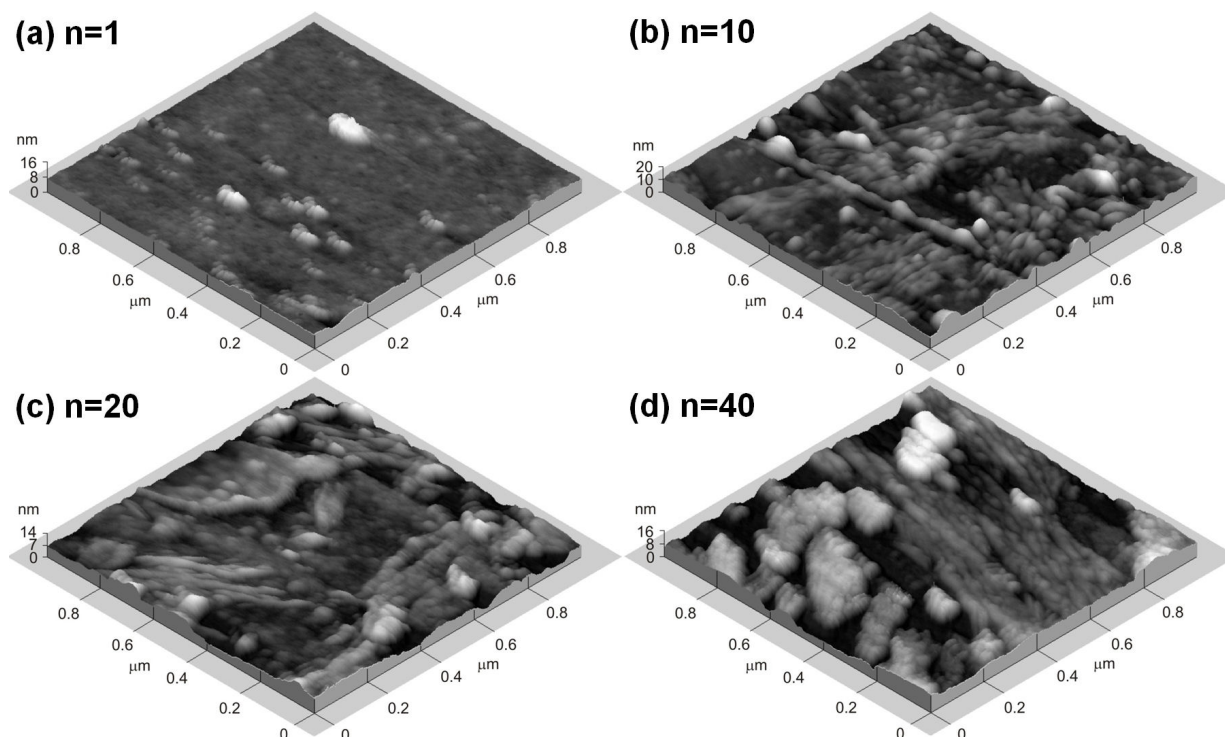


FIGURE 6. 3D-AFM micrographs showing the surface morphology of deposited LB-films: a) A monolayer ( $n = 1$ ) bent-core based LB-sample, b) A multilayered ( $n = 10$ ) LB-sample, c) A multilayered ( $n = 20$ ) LB-sample and c) A multilayered ( $n = 40$ ) LB-sample, respectively.

creased roughness (20.1 Å) and inter-grain porosity. This points to severe difficulties for the optimal packing of this kind of asymmetric compounds to form homogeneous multi-layered systems as the number of depositions increases. Finally, in the case of excessive number of deposited layers ( $n = 20 - 40$ , see Fig. 6/c-d), the formation of fully randomly multi-shaped structures with lengths ranging from 50 to 200 nm takes place. These extremely chaotic systems formed by greater rounded, flattened or worm-like structures grow randomly forming very inhomogeneous arrangements with highest roughness (up to 27.6 Å). The microscopic inter-granular space and porosity are substantially increased leading to a substantial decrease of the LB-film quality as several imperfections and dispersed particles can be identified on the film surface. It is therefore suggested that the observed disorder promotes a poor molecular orientation in the upper layers and consequently, a loss of the deposited material, supporting the extreme decrease in the absorption spectra as observed in Fig. 5.

### 3.4. NLO/SHG-properties

Regarding the NLO-properties, the LB-deposition technique has been commonly implemented as a practical alternative to electrically poled spin-coated organic films in order to create oriented non-centrosymmetric molecular systems of push-pull NLO-chromophores for SHG-applications. This condition was satisfactorily achieved by our Z-type mono- and multi-layer LB-systems as required for quadratic NLO-effects [19-20]. In fact, in this study conventional transmission angle-dependent SHG measurements were performed in both the P-In/P-Out and S-In/P-Out laser beam polarization geometries, these measurements were carried out for increasing number of deposited LB-layers in order to verify non-centrosymmetric Z-type ordering (for  $n$ : 1, 5, 10, 15, 20 and 40 LB-layers). As expected, negligible SHG-signals were measured for the amorphous glass substrate and the SHG-intensities of the LB-layers were found to be about 60-70% stronger for the P-In/P-Out implemented geometries compared to the S-In/P-Out ones. As shown in Fig. 7/a-b, the angle-dependent Maker fringe patterns of the asymmetric ABLC based mono- and multi-layered LB-structures, essentially exhibit a major contribution of two tensorial coefficients measured by the P-In/P-Out and S-In/P-Out polarizing geometries, namely the  $\chi_{zxz}^{(2) \prime}$  and  $\chi_{zzz}^{(2) \prime}$  coefficients, which makes evident the anisotropy of these film structures. Indeed, the SHG-activity of the samples as a function of the incidence angle (Fig. 7/a-b) can be clearly appreciated. The deficiency of SHG-signals at normal laser incidence and the SHG-intensity augment with increasing incident angles represent typical features of stable and homogeneous molecular alignment within the LB-structure. The intense SHG-activity detected for the P-In/P-Out (fundamental-input/SHG-output) beam polarization geometries is due to optimal optical polarization matching between the fundamental beam polarization (electric field) and the permanent molecular dipole moment

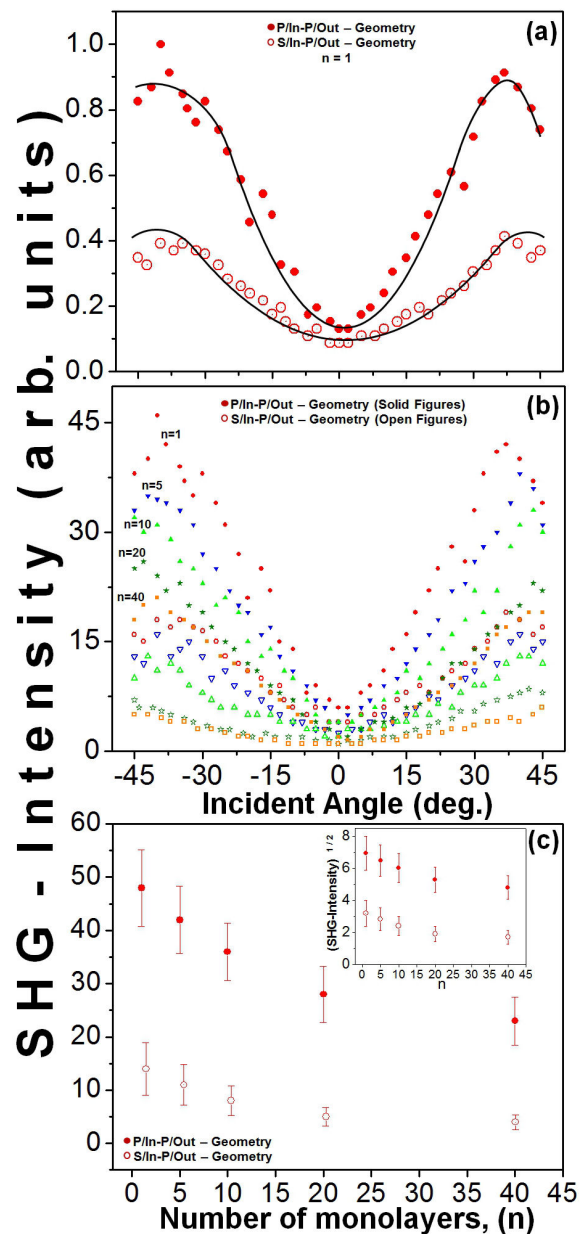


FIGURE 7. a) Representative angular dependence of the SHG-intensity for: a) the monolayer LB-surface ( $n = 1$ , normalized SHG-intensity, solid lines: theoretical fitting), b) multi-layered ( $n = 1, 5, 10, 20$  and  $40$ ) LB-film samples (solid/filled figures: NLO-measurements taken for the P/In-P/Out polarizing geometry, open symbols: NLO-measurements taken for the S/In-P/Out geometry) and c) SHG-maxima dependence on the number of deposited LB-layers (at optimal phase-matching conditions for P/In-P/Out and S/In-P/Out polarization geometries). Inset figure: square-root of the SHG-intensity maxima as a function of the number of deposited layers.

$\vec{P}_{NET}$  located between the two main ABLC molecular axes (see Fig. 1/b). With the aim of performing an estimation of the most significant NLO-coefficients under our experimental restrictions, we related these coefficients, in this simplified case, to the net molecular polarization axis  $\vec{P}_{NET}$ ,

where the polar 2D-bent-core compound may play the role of a push-pull rod-like structure, being the main NLO-direction assigned, in this case, to the short molecular axis  $z'$  (vectorially corresponding to the polar direction:  $\chi_{zzz}^{(2)'}$ -component). Particularly, Fig. 7/b-c shows the strongest SHG-signals generated by each mono/multilayer sample at incidence angles within the 39-45° interval. At these incident angles, maximal fundamental molecular excitations can be achieved (optimal phase-matching condition). This is due to the perpendicular-close  $\vec{P}_{NET}$  polar alignment achievable by these bent-molecules under the special Z-type LB-architecture, *i.e.* the net molecular polar axis  $\vec{P}_{NET}$  pointing outwards the substrate plane.

The Maker fringes data allowed us, under certain considerations, to estimate the macroscopic  $\chi_{zxx}^{(2)'}$  and  $\chi_{zzz}^{(2)'}$  independent tensorial components for the effective one-polar-axis bent-core based LB-films, assuming the simplified rod-like analysis. By continuously monitoring the SHG-response from the mono- and multi-layer LB-structures, we confirmed that neither fundamental wave induced damage nor molecular desorption occurred in the LB-layers. In general, the average NLO-effective macroscopic coefficient  $\chi_{eff}^{(2)'}$  of a given material can be estimated in a simple way by directly comparing the SHG-signals of the sample with those obtained from a reference material under similar experimental conditions (in this case the  $d_{11}$ -wedged  $\alpha$ -quartz crystal). A simple equation allowed us to provide a relative estimation for the macroscopic  $\chi_{eff}^{(2)'}$ -effective nonlinear optical susceptibility of the studied sample, by directly comparing the quadratic intensity dependence between the SHG signal of the reference crystal and that observed for the sample under study. Eq. (1) represents this quadratic dependence for the developed LB-films:

$$I_{2\omega}^{LB-Film} \propto I_{\omega}^2 (l_c^{LB-Film} \chi_{eff}^{(2)'-LB-Film})^2 \times \sin^2 \left[ \frac{\pi l^{LB-Film}}{2l_c^{LB-Film}} \right], \tag{1}$$

where  $l_c^{LB-Film}$  represents the coherence length of the LB-film sample and  $l^{LB-Film}$  is the LB-sample thickness. Note that for the present case, the thickness of the mechanically stable molecular monolayer is much smaller than the intrinsic coherence length of the specimens (in the range of a few microns), under this limit ( $l^{LB-Film} \ll l_c^{LB-Film}$ ), the relation between the generated SHG-intensity and the intensity of the fundamental wave may be expressed according to the following expression:

$$I_{2\omega}^{LB-Film} \propto I_{\omega}^2 \left[ (\pi/2) l^{LB-Film} \chi_{eff}^{(2)'-LB-Film} \right]^2$$

This follows the NLO-calibration using the reference crystal, which can be reasonably applied for any selected polarizing geometry:

$$\chi_{eff}^{(2)'-LB_{p-p,s-p}} \propto \chi_{11}^{(2)-Quartz} \left( \frac{2l_c^{Quartz}}{\pi l^{LB-Film}} \right) \times \left[ \frac{I_{2\omega}^{LB}}{I_{2\omega}^{\chi_{11}^{(2)-Quartz}}} \right]^{1/2} \tag{2}$$

here,  $I_c^{Quartz}$  is the coherence length of the reference quartz crystal ( $\sim 22 \mu\text{m}$ ),  $I_{2\omega}^{\chi_{11}^{(2)-Quartz}}$  and  $I_{2\omega}^{LB}$  are the SHG-peak intensities (at maximum of the Maker fringes observed for both the reference crystal and LB-sample, respectively). In this case, modeling our sample as a three-layer structure Air  $\rightarrow$  LB-Film  $\rightarrow$  Substrate, we have obtained, after simultaneous fitting the  $I_{2\omega}^{p-p}$  and  $I_{2\omega}^{s-p}$  signals, as function of the corresponding  $\chi_{eff}^{(2)'p-p,s-p}$  coefficients, and the effective incident angle of the fundamental wave [23], the NLO-coefficients for the monolayer ( $n = 1$ ) sample, namely:  $\chi_{33}^{(2)} \equiv \chi_{zzz}^{(2)} \approx 9.1 \text{ pm V}^{-1}$  and  $\chi_{31}^{(2)'} \equiv \chi_{zxx}^{(2)'} \approx 5.3 \text{ pm V}^{-1}$  ( $\chi_{ij}^{(2)'}$  in contracted notation). The nonlinear theoretical fit to the envelope (implementing a least square minimization procedure, see Fig. 7/a), neglecting any correction for the local field factors, provided the values of the main tensorial components  $\chi_{ij}^{(2)'}$  of the LB-monolayer sample.

On the other hand, the single LB-monolayer and macroscopic SHG-measurements permit, under the rod-like polar approximation, the analysis of several physical properties of these bent-core compounds at the microscopic molecular level, such as the molecular hyperpolarizability tensor  $\beta^{(2)}$ , or the corresponding polar orientational parameter ( $S_P$ ), and subsequently an effective polar molecular orientational angle  $\theta_{eff}^p$  with respect to the substrate's normal. Indeed, under our particular rod-like approximation, the  $S_P$  parameter can be defined through the  $\chi_{33}^{(2)'}/\chi_{31}^{(2)'}$  ratio for the 1D-molecular polar-axis of the bent-core compound [25]. We take advantage of this possibility in order to evaluate the  $S_P$  parameter, which gives in this simplified case, a direct estimation of the average polar molecular alignment within the LB-monolayer system. In the case where an isotropic polar-axis orientational distribution around the film's normal axis is assumed (condition easily verified from the negligible<sup>i</sup> SHG-signals measured at normal laser incidence for both the P-In/P-Out and S-In/P-Out polarizing geometries), the SHG reaches its maximum with varying incidence angle  $\theta$ . This condition is reasonably achieved by the P/In-P/Out polarizing geometry as the fundamental beam electric field inside the film becomes nearly parallel to the molecular polar-axis at an adequate angle of incidence. Thus, according to Refs. [25-26], the averaged polar orientational parameter can be defined as:

$$S_P \approx \frac{\chi_{33}^{(2)'}/\chi_{31}^{(2)'}}{2 + \chi_{33}^{(2)'}/\chi_{31}^{(2)'}} \approx \cos^2 \theta_{eff}^p.$$

According to our particular rod-like polar approximation we found for the 1D-polar/2D-molecules that the polar-axis orientation of the ABLC-based LB monolayer ( $n = 1$ ) is given by  $S_{ML_{n-1}}^p \approx 0.462$  (corresponding to:  $\theta_{eff}^p \approx 47.2^\circ$ ). This angle indicates that the average molecular polar axis

(director-vector) is actually closer to the substrate surface, in agreement with our molecular modeling.

Similarly, according to the implemented approximations and from our previous results it is also possible to estimate an effective molecular hyperpolarizability coefficient  $\beta_{\text{eff}}^{(2)}$  along the macroscopic polar axis as function of the  $S_P$  parameter, taking into account the macroscopic  $\chi_{ij}^{(2)'$ -coefficients and the surface density of active chromophores  $N_S$  (molecules  $\text{m}^{-2}$ ), as described in the following expressions [25-26]:

$$\beta_{\text{eff}}^{(2)} \cong \chi_{33}^{(2)'} / (N_S S_p^{3/2}), \quad (3)$$

$$\beta_{\text{eff}}^{(2)} \cong \chi_{31}^{(2)'} / (N_S S_p^{1/2})(1 - S_p). \quad (4)$$

According to these equations and from the experimental results shown in Figs. 2-3, the molecular area in the monolayer was  $\sim 91 \text{ \AA}^2$ . Since the spot-size of the focused laser beam was  $\varnothing \approx 60 \text{ \mu m}$ , the  $N_S$  parameter is in the order of  $N_S \approx 6.2 \times 10^9$  molecules  $\text{m}^{-2}$ . Hence, an estimated value of  $\beta_{\text{eff}}^{(2)} \cong 408 \times 10^{-21}$  esu can be straightforwardly determined. Despite this effort, the hyperpolarizability  $\beta_{ijk}^{(2)}$ -tensorial components still remain inaccessible to investigations limited to transmission single beam SHG-experiments and cannot be directly established from this approximation. In order to further estimate, under the present circumstances, the  $\beta_{ijk}^{(2)}$ -components, we implement concluding remarks from another model based on surface second harmonic generation (SSHG) measurements, which has been applied and verified specifically for 2D charge-transfer bent-core mesogens [5]. In general, this model establish that the first hyperpolarizability  $\beta^{(2)}$  of bis-dipolar compounds can be expressed in terms of the hyperpolarizabilities  $\beta_{\xi\xi\xi}^{(2)}$  of the one-dimensional monomeric units and the dihedral angle  $\Theta$  between the two constituting monomers [5,27]; thus, the  $\beta_{ijk}^{(2)}$ -components of the 2D-bis-dipolar molecule can be analyzed by the superposition of the monomeric contributions. Assuming here, for a straightforward analysis, the simplified axial  $C_{2V}$ -symmetry approximation, generally accepted for this kind of compounds under ferroelectric polar arrangements (including LB-monolayers and prepared EO-film cells [5,28-29]), and taking into account the one-dimensional monomeric unit approximation, the nearly rod-like shape of these molecules and the net molecular polarization axis  $\vec{P}_{NET}$ , there are only four nonvanishing  $\beta_{ijk}^{(2)}$ -components to evaluate [5,14]:

$$\beta_{333}^{(2)} = 2 \cos^3(\Theta/2) \beta_{\xi\xi\xi}^{(2)}, \quad (5)$$

$$\beta_{311}^{(2)} = \beta_{131}^{(2)} = \beta_{113}^{(2)} = 2 \cos(\Theta/2) \sin^2(\Theta/2) \beta_{\xi\xi\xi}^{(2)} \quad (6)$$

Thus, we can at least evaluate the ratio of the two independent  $\beta_{ijk}^{(2)}$ -tensorial components as  $\beta_{311}^{(2)} / \beta_{333}^{(2)} = \tan^2(\Theta/2)$ . This ratio is about  $\beta_{311}^{(2)} / \beta_{333}^{(2)} \approx 2.7$ , which is in the same order of magnitude of other calculations performed for bent-core mesogens [5].

On the other side, considering the multilayered structures and according to original experimental studies concern-

ing SHG in organic LB-structures [30-33], the Z-type LB-samples may exhibit a quadratic relation between the observed SHG-intensity and the number of layers deposited. In fact, in the most general and optimal case, the nonlinear susceptibility of the system can be expressed as a sum of contributions from the substrate surface  $\chi_s^{(2)}$  and from the deposited multilayer  $\chi_{ML}^{(2)}$  nonlinear susceptibilities, respectively. That is:  $I_{2\omega} \propto |\chi_s^{(2)} + \chi_{ML}^{(2)}|^2 I_\omega^2$ . For perfectly aligned LB-multilayers,  $\chi_{ML}^{(2)}$  is proportional to the number of deposited layers  $n$  and as a result, a quadratic dependence according to  $I_{2\omega} \propto n^2$  should be expected as a linear increase in a  $\sqrt{I_\omega^2}$  vs.  $n$  plot [19-21,30,34]. However, as shown in Fig. 7/c (inset), this approximation is not satisfied for our studied ABLC-based LB-arrays. Instead, a nearly linear decrease on the SHG-response with the number of layers is observed, in common agreement with the absorption measurements at 286 nm. In general, the experimental data may deviate from this approach for excessive multilayer depositions, where the system may drastically turn into a mechanically unstable configuration. Up to date, only a few studies of monolayer symmetric and asymmetric bent-core based LB-systems have been reported in the literature [5-6,8-9,12,35] and one successful study of multilayer bent-core based LB-systems performed by our group in symmetric bent-core systems [13]. Indeed, the improvement of multilayer LB-systems with bent-core "banana" compounds seems to be a challenging task of current interest, since a drastic collapse of an excessive number of deposited layers seems to occur for this kind of compounds. On the other hand, according to several reports, the structural properties and chemical substituents of the implemented molecular systems may also play an important role in the stability of LB-multilayer arrangements [2,20,30-31]. This is in fact the case for the implemented asymmetric bent-core compound bearing two significantly long  $\text{OC}_{12}\text{H}_{25}$  alkyloxy end-chains per molecule, where according to our geometrical modeling performed for the compound-water interface, the assumption of a layer molecular ordering with the respective net polarization and molecular wings aligned outwards the substrate plane, is well supported. Hence, we argue that the alignment and mechanical stability of the multilayered LB-films drastically drops for increasing number of molecular depositions. This is partially due to the excessive length of the two alkyloxy molecular end-chains which, under the assumed asymmetric configuration, the presence of such long units contributes to an unstable structural configuration for an excessive number of layers. In this case, the polar groups from the upper layers cannot compensate the molecular dipole-dipole interactions as the connection with the substrate loses its influence; as a result, disorder in the upper layers increases considerably in comparison to the lower ones, material loss take place and the absorption and SHG response are drastically diminished [30-31,36]. Indeed, as shown in Fig. 7/c and according to the polar nature of these molecules and Fig. 3, it is very possible that the first  $n = 1 - 10$  deposited layers fully accomplish the

Z-type architecture with an in-plane perpendicular-close polar orientation. However, according to Zou *et al.* [9], disorder of the upper layers may be visualized in many configurations, even for banana-molecules in stable configurations keeping both core and end-groups quite flat on the surface. Such configurations depend on molecular packing and density producing herringbone patterns with the two end-chains fitting into the bow-shaped core (for dense configurations) or forming layered structures with alternating polarity for consecutive in-layer molecules (for less dense configurations). In both cases, a drastic decrement of the quadratic NLO-properties is expected due to the cross-cancellation of the SHG-response or loss of symmetry. In fact, in our case, the dense molecular packing required for LB-deposition has led to unstable multilayered LB-architectures; thus, a consistent correlation between the obtained SHG-response and absorbance spectra of the multilayered LB-films was obtained. Finally, the AFM-results agree reasonably well with the absorbance and NLO-optical measurements given that for increasing molecular disorder, as observed in the different AFM-textures of excessive multilayered LB-systems, both the SHG and linear absorption signals, accordingly, decrease. Again, this is attributed to the randomly oriented upper molecular layers, the loss of structural symmetry and material accumulation, respectively.

#### 4. Conclusions

In this work, we have demonstrated that it is possible to fabricate stable monolayer LB-films from an asymmetric fluorine substituted bent-core liquid-crystalline compound, and multilayered systems for at least a moderate number of deposited layers ( $n \leq 10$ ). This result is interesting from a fundamental perspective, since the molecular ordering of complex bent-core compounds may, in principle, be studied in more detail in these discrete nanostructured layers.

The optimal conditions for LB-deposition were exhibited via BAM- and Surface pressure-molecular area isotherms-measurements. According to the most probable conformation of the implemented ABLC-compounds after deposition of LB-films on glass substrates, the assumption of a layer molecular ordering with the central hydrophilic benzene-core in contact with the glass substrate and the respective net polarization homogeneously aligned outwards the substrate plane, is in fact well supported. This was actually verified by NLO/SHG-measurements. Indeed, we presented a simplified SHG-analysis based on the assumption of a homogeneous molecular polar-axis alignment (rod-like approximation) which is reasonable due to the inherent 2D-geometrical structure and 1D-polar configuration of the ABLC-mesogens. This kind of media allows molecular ordering inspections by indirectly monitoring their respective polar axis distribution, as has been previously proven by scanning NLO-SHG-microscopy [15,17,37]. Accordingly, P-In/P-Out and P-In/S-Out angle dependent SHG-measurements were performed in ABLC-based monolayer LB-systems allowing the

estimation of the average molecular orientational polar order and the main macroscopic NLO-coefficients of this system which are in good agreement with those reported in the literature for bent-shaped compounds composed of several benzene rings. So far, most of the investigations performed in bent-core liquid crystalline based LB-films according to the SHG-technique, have been carried out in monolayer systems; in this work we have proven that it is also possible to develop multilayered Z-type LB-films with quadratic NLO-response for at least a moderate number of layers implementing the asymmetric ABLC-mesogen, where the film structure can still exhibit an adequate structural architecture. As a matter of fact, absorbance spectroscopy, SHG-measurements and AFM-morphology inspections have demonstrated a homogeneous decrease of material deposition for increasing multilayer depositions, where the system drastically turns into a mechanically unstable structure, indicating a poor LB-architecture achievable for these asymmetric ABLC-based LB-systems. Indeed, even though material accumulation occurs for the first 5-10 layers as verified via optical absorption measurements; NLO-measurements (see Fig. 7/c) reveals that the SHG-efficiency is not only affected by the material loss, but by the molecular disorder occurring from the earliest deposited layers which play an important role in the subsequent structural collapse.

Certainly, the improvement of multilayered LB-systems implementing bent-core "banana" compounds seems to be a challenging task of current interest which has to be further investigated in order to improve the film quality for optical and photonic applications. Future studies concerning the selection of different kind of substrates, molecular aggregation conditions and the optimization of the molecular concentration within the precursor solvent-chromophore Langmuir-film system should be performed in order to improve the multilayer ordering, and the NLO-response of deposited ( $n > 10, 30...$ ) LB-layers with several symmetric and asymmetric bent-core compounds, respectively. This task is very important since it has been observed that asymmetric bent-core molecular structures exhibit significant NLO/SHG effects and potential EO-applications [38-39]. Additionally, a more detailed NLO-analysis will be necessary in order to finely tune the NLO-coefficients; this will be performed in future works according to the theory developed in Ref. [5] for two-dimensional bis-dipolar molecules.

#### Acknowledgments

The authors wish to thank to Martín Cruz Villafañe for technical assistance (ICN-UNAM) and to J. Guadalupe-Bañuelos (CCADET-UNAM) for AFM-imaging. Financial support from DGAPA-PAPIIT-UNAM (projects IN111711, PE213912 and IG100713) is also gratefully acknowledged. O.G. Morales-Saavedra acknowledges financial support from the DAAD academic organization and from the LC Halle-group (Germany).

- i.* Residual surface generated SHG allow the detection of small signals at normal incidence.
1. G. Pelzl, G.S. Diele, and W. Weissflog, *Adv. Mater.* **11** (1999) 707.
  2. Y. Tang, Y. Wang, G. Wang, H. Wang, L. Wang, and D. Yan, *J. Phys. Chem. B* **108** (2004) 12921.
  3. A. Jákli, D. Krüerke, H. Sawade, L.C. Chien, and G. Heppke, *Liq. Cryst.* **29** (2002) 377.
  4. A. Jákli, D. Krüerke, and G.G. Nair, *Phys. Rev. E* **67** (2003) 051702.
  5. Y. Kinoshita, B. Park, H. Takezoe, T. Niori, and J. Watanabe, *Langmuir* **14** (1998) 6256.
  6. L.M. Blinov *et al.*, *Appl. Phys. Lett.* **87** (2005) 241913.
  7. G.J. Ashwell, and M.A. Amiri, *J. Mater. Chem.* **10** (2002) 2181.
  8. J.W. Baldwin *et al.*, *J. Phys. Chem. B* **106** (2002) 12158.
  9. L. Zou *et al.*, *Langmuir* **20** (2004) 2772.
  10. S. Henon, and J. Meunier, *Rev. Sci. Instrum.* **62** (1991) 936.
  11. D. Hönig, and D.J. Möbius, *Phys. Chem.* **95** (1991) 4590.
  12. J. Wang, L. Zou, A. Jákli, W. Weissflog, and E.K. Mann, *Langmuir* **22** (2006) 3198.
  13. P. García-Vázquez, O.G. Morales-Saavedra, G. Pelzl, and M.P. Carreón-Castro, *Thin Solid Films* **517** (2009) 1770.
  14. M.W. Schröder, G. Pelz, U. Donemann, and W. Weissflog, *Liq. Cryst.* **31** (2004) 633.
  15. H. Takezoe, and Y. Takanishi, *Jpn. J. Appl. Phys.* **45** (2006) 597.
  16. H.S. Nalwa, T. Watanabe, and S. Miyata, *Adv. Mater.* **7** (1995) 754.
  17. O.G. Morales-Saavedra, A. Jákli, G. Heppke, and H.J. Eichler, *J. Nonlinear Opt. Phys. Mater.* **15** (2006) 287.
  18. American society for testing and materials, ASTM Standard D1193 (2006) "Specification for Reagent Water", ASTM International, West Conshohocken, PA, [www.astm.org](http://www.astm.org).
  19. P.N. Prasad and D.J. Williams, *Nonlinear Optical Effects in Molecules and Polymers* (New York: Wiley; 1991).
  20. H.S. Nalwa and S. Miyata (Eds.), *Nonlinear Optics of Organic Molecules* (Boca Raton Florida: CRS Press Inc; 1997).
  21. F. Kajzar and J.D. Swalen (Eds.), *Organic thin films for waveguiding nonlinear optics* (San Jose CA: Gordon and Breach Publishers; 1996).
  22. S.R. Marder, J.E. Sohn and G.D. Stucky, *Materials for nonlinear optics, chemical perspectives* (Washington, D.C.: ACS Symposium series 455, American Chemical Society; 1991).
  23. R.W. Boyd, *Nonlinear optics* (San Diego CA: Academic Press; 1992).
  24. N. Duff, J. Wang, E.K. Mann, and D.J. Lacks, *Langmuir* **22** (2006) 9085.
  25. A. Leray, D. Rouède, C. Odin, Y. Le Grand, O. Mongin, and M. Blanchard-Desce, *Opt. Commun.* **247** (2005) 213.
  26. A. Leray *et al.*, *Langmuir* **20** (2004) 8165.
  27. H.J. Deussen *et al.*, *J. Am. Chem. Soc.* **118** (1996) 6841.
  28. R. Macdonald, F. Kentischer, P. Warnick, and G. Heppke, *Phys. Rev. Lett.* **20** (1998) 81.
  29. A. Eremin, S. Diele, G. Pelzl, H. Nadasi, and W. Weissflog, *Phys. Rev. E* **67** (2003) 021702.
  30. S. Schrader *et al.*, *Mater. Sci. Eng. C* **8** (1999) 527.
  31. G. Roberts (Ed.), *Langmuir-Blodgett Films* (New York: Plenum Press; 1990).
  32. S.G. Davis, M.E. C. Polywka, T. Richardson, G.G. Roberts, Br. Patent. No. 8717566 (1988).
  33. G. Decher, B. Tieke, G. Bosshard, and P. Gunter, *Ferroelectrics* **91** (1989) 193.
  34. E. Rivera, M.D.P. Carreón-Castro, L. Rodríguez, G. Cedillo, S. Fomine, and O.G. Morales-Saavedra, *Journal of Dyes and Pigments* **74** (2007) 396.
  35. I. Giner, I. Gascón, J. Vergara, M.C. López, M.B. Ros, and F.M. Royo, *Langmuir* **25** (2009) 12332.
  36. I. Robinson, J.R. Sambles, and N.A. Cade, *Thin Solid Films* **178** (1989) 125.
  37. O.G. Morales-Saavedra, M. Bulat, S. Rauch, and G. Heppke, *Mol. Cryst. Liq. Cryst.* **413** (2004) 607.
  38. M.B. Ros, J.L. Serrano, M.R. de la Fuente, and C.L. Folcia, *J. Mater. Chem.* **15** (2005) 5093.
  39. J. Etxebarria, and M.B. Ros, *J. Mater. Chem.* **18** (2008) 2919.